Numerical Simulation of Inclusion Removal in a Novel Tundish with Swirl Flow

Jianchuan Yan, Tao Li and Jun Liu

Abstract It is of great importance to remove the inclusions as much as possible in the molten steel. The inclusion collision rate is significantly improved by generating centrifugal flow in the tundish with an electromagnetic device, which induces the inclusions to grow and float. However, the electromagnetic device requires an external equipment component that is difficult to maintain. Additionally, a turbulence inhibitor is commonly used to optimize the turbulence flow in the tundish. This paper describes a novel tundish design with a turbulence inhibitor that generates swirl flow in a cylindrical zone, which produced an effect similar to the electromagnetic device. The gravitational potential energy of the molten steel from the nozzle is converted into kinetic energy of the swirling flow in the tundish. The inclusion removal rates with various nozzle diameters were investigated, and the optimal turbulence inhibitor size and structure were identified by numerical simulation.

Keywords Tundish · Inclusion removal · Turbulence inhibitor
Numerical simulation · Centrifugal flow

Introduction

In steelmaking, nonmetallic inclusions are mainly generated during deoxidization process or originate with the refractory materials; these inclusions are of great harm to the quality and mechanical properties of the steel products [1]. To improve the quality of the molten steel, many methods to reduce inclusion formation and

J. Yan · T. Li (✉) · J. Liu
College of Materials Science and Engineering, Chongqing University,
Chongqing 400044, People's Republic of China
e-mail: litao0518@hotmail.com

T. Li
Chongqing Key Laboratory of Vanadium-Titanium Metallurgy and Advanced Materials,
Chongqing University, Chongqing 400044, People's Republic of China

remove inclusions have been investigated [2]. In the continuous casting process, a tundish acts not only as a buffer and distributor between ladle and casting mold, but also plays an important role in the removal of inclusions [3]. Studies of the flow characteristics of molten steel in the tundish are of great significance to improve the quality and productivity of steel products. Inclusion separation is abetted by increased residence time, elimination of dead zones and smooth molten steel flow fields. Various flow control devices have been put into application, including bubble curtains, weirs, dams, baffles and turbulence inhibitors [4]. Kawasaki Steel proposed a Centrifugal Flow Tundish (CFT) [5], which could generate centrifugal flow in the rotating chamber of the tundish driven by an external electromagnetic field. The CFT method has proved to effectively eliminate inclusions; inclusion removal is accomplished by increasing residence time and the collision rate of inclusion particles in the centrifugal flow [6]. However, the CFT is not widely applied due to its requirements of the external electromagnetic device and energy consumption.

In this paper, a novel tundish is proposed based on the idea of a CFT installed with an innovative turbulence inhibitor to generate swirling flow. The turbulence inhibitor could obtain the similar effect to the electromagnetic device in the CFT without the requirements of external device and electricity consumption. Furthermore, it is cost efficient and easy to be maintained and replaced. The size and structure of the novel tundish are optimized through computational fluid dynamics (CFD) simulation implemented by ANSYS Fluent in the current work.

Model Description

Tundish Model

The novel tundish differs from tradition by employing the turbulence inhibitor that is designed as a hollow cylinder with an inlet from its top surface and two tangential outlets located symmetrically around the side wall of the cylinder (See Fig. 1b). The tangential outlets generate swirling flow in the rotating chamber (See Fig. 1a) of the tundish. The gravitational potential energy of the molten steel from the nozzle is converted to kinetic energy of the swirling flow in the rotating chamber. The turbulence inhibitor will be called the "swirling flow generator" in the following text. The components and planes of the tundish are labelled in Fig. 1. These cross sections Plane 1 and Plane 2 are parallel to the bottom surface of the tundish. Plane 1 is located at 125 mm above the bottom of the tundish, which is going through the middle of the outlet of the swirling flow generator. While Plane 2 is located at 275 mm above the bottom of the tundish, which is between the upper surface of the swirling flow generator and the nozzle outlet.
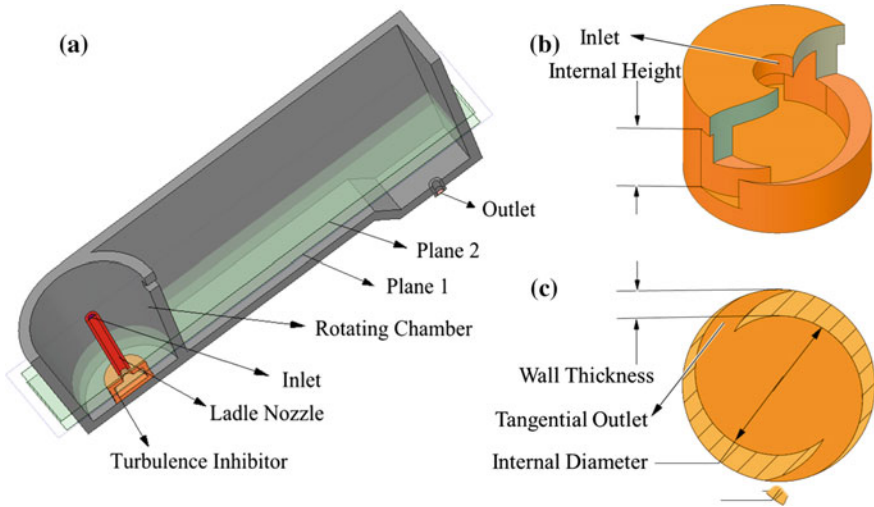
Fig. 1 Structure and components of the tundish. **a** Components of the tundish. **b** and **c** Structure of the swirling flow generator

The three-dimensional (3D) model of a simplified tundish installed with a swirling flow generator is established. The detailed geometry and parameters are shown in Fig. 2, in which the internal diameter of the swirling flow generator is variously changed and optimized in the following discussions.

Numerical Simulation

Numerical simulations were carried out by using the commercial software ANSYS FLUENT 18.0® , which was widely applied in the field of the numerical simulation of the flow fields in the tundishes [7–10]. In this study, the meshes of the 3D tundish models are produced by ICEM with the same operating process for each tundish model. The total quantity of the grids is approximately 1.7 million. The calculations are considered to have converged as the residual of all the variables are below 1×10^{-3}. The numerical simulations were carried out based on the following consumptions to simplify the simulation model:

(1) The molten steel is a Newtonian incompressible fluid. The density and viscosity of the molten steel are constants, which are 7080 kg/m^3 and 0.0055 kg/(m s), respectively.
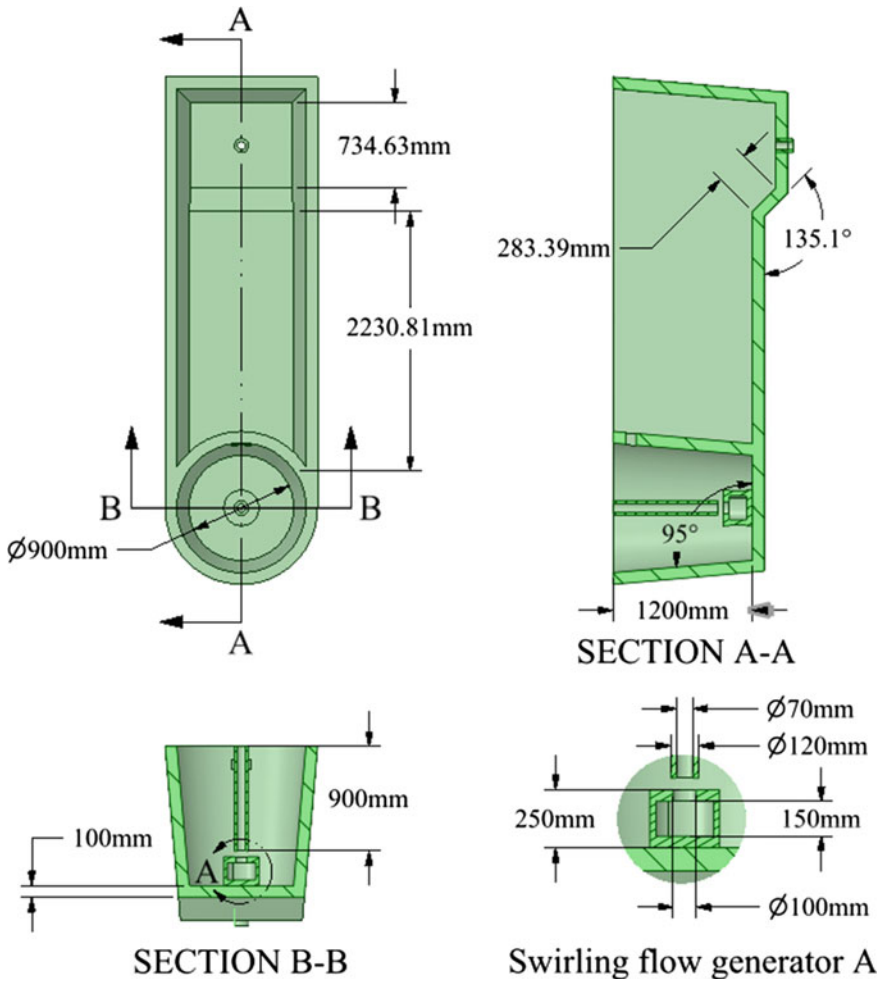(2) The temperature and compositions of steel within the tundish are assumed to be homogenously distributed.

Fig. 2 Dimensions of the three-dimensional model

(3) The walls of the tundish are considered as smooth wall.
(4) Regardless of the influence of the slag phase, the top surface of the molten steel is set to be specified shear wall boundary condition.
(5) The inclusion particles are assumed to be spherical with the density of 3000 kg/m³.

Turbulence Model

The renormalization group (RNG) k-ε two-equation turbulence model is adopted in this work based on the previous study [11]. The governing equations for the steady flow are solved within a finite control volume are presented as follows.

The continuity equation of the fluid is,

$$\frac{\partial u_i}{\partial x_i} = 0 \tag{1}$$

The momentum conservation equation is given by,

$$\rho \frac{\partial (u_i u_j)}{\partial x_j} = -\frac{\partial p}{\partial x_i} + \frac{\partial}{\partial x_j}\left[\mu_{eff}\left(\frac{\partial u_i}{\partial x_j} + \frac{\partial u_j}{\partial x_i}\right)\right] \tag{2}$$

The turbulence kinetic energy ε can be derived from the following equation,

$$\rho\left(\frac{\partial}{\partial x_j}\right)\left(u_j k - \frac{u_{eff}}{\sigma_k} \times \frac{\partial k}{\partial x_j}\right) = G - \rho\varepsilon \tag{3}$$

The dissipation rate k is calculated by the following formula,

$$\rho \frac{\partial (u_j \varepsilon)}{\partial x_j} = \frac{\partial}{\partial x_j}\left(\frac{u_{eff}}{\sigma_\varepsilon} \times \frac{\partial \varepsilon}{\partial x_j}\right) + \frac{(C_1 G\varepsilon - C_2 \rho\varepsilon^2)}{k} \tag{4}$$

where, C_1, C_2, σ_ε and σ_k are constants recommended by Launder and Spalding [12]; and G is given by,

$$G = \mu_t \frac{\partial u_j}{\partial x_i}\left(\frac{\partial u_i}{\partial x_j} + \frac{\partial u_j}{\partial x_i}\right) \tag{5}$$

The effective viscosity is modified by,

$$\mu_{eff} = \mu\left(1 + \sqrt{\frac{C_\mu}{\mu}\frac{k}{\sqrt{\varepsilon}}}\right)^2 \tag{6}$$

Inclusions Tracking Model

The capacity to separate inclusion particles from molten steel is one of the most important criteria in the optimization of the tundish structure. The discrete phase model (DPM) is introduced to simulate the motion of the inclusion particles in the phase of the molten steel, and thus calculate the removal rate of the inclusion particles. In the discrete phase model, the boundary condition of the outlet of the tundish is set to be "escape", which means that the inclusion particles could exit from the outlet with the molten steel. The boundary condition of the top surface of the tundish is set to be "trap", where the inclusion particles become trapped. The boundary conditions at all of the other tundish walls are set to be "reflect", where the inclusion particles are reflected back into the molten steel after they collide with those walls.

Results and Discussion

Comparison Between Novel and Traditional Tundishes

The molten steel flow in the tundishes was simulated with the swirling flow generator and the traditional turbulence inhibitor (200 mm internal diameters in both devices) to illustrate the function of swirling flow generator. Figure 3 compares the molten steel streamlines in the two models. With the swirling flow generator, an obvious circular motion of the molten steel is found in the cylindrical rotating chamber. The velocity contours of the cross section A-A (See Fig. 2) are shown in Fig. 4. The velocity of the molten steel in the tundish with the swirling flow generator is much more symmetric than that with the traditional turbulence inhibitor. It is clear that a swirling flow is created in the rotating chamber by guiding the molten steel from the nozzle to flow out of the tangential outlets.

Fig. 3 Streamlines of tundishes with traditional turbulence inhibitor and swirling flow generator


(a). Traditional turbulence inhibitor

(b). Swirling flow generator
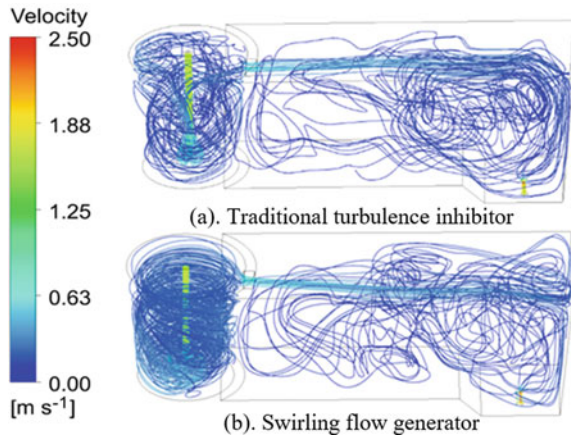
Fig. 4 Velocity contours in section A-A of tundishes with traditional turbulence inhibitor and swirling flow generator

(a). Traditional turbulence inhibitor

(b). Swirling flow generator
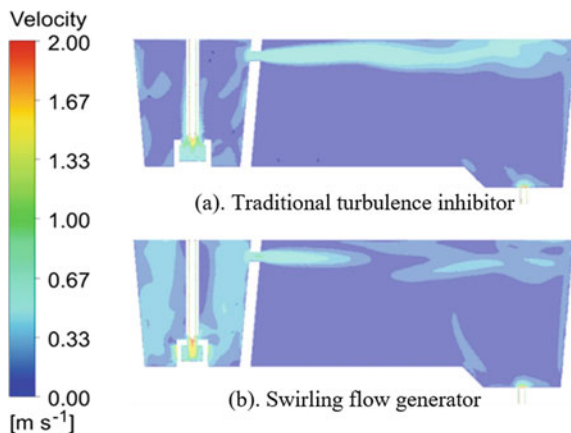
Influence of Nozzle Length

Two tundish models are established to clarify the influence of the immersing depth of the 250 mm internal diameter nozzle. The model of case (a) shown in Fig. 5a is designed exactly following the parameters shown in Fig. 2. The immersion depth of the nozzle is 900 mm, which is positioned 50 mm above the inlet of the swirling flow generator. The immersion depth is increased to 970 mm in case (b) shown in Fig. 5, in which the nozzle is put into the swirling flow generator. The streamlines and the velocity contours of the molten steel are shown in Figs. 5 and 6. The streamlines of the molten steel in the tundish become more disordered and asymmetrical when the nozzle immersion depth is extended from 900 to 970 mm. Meanwhile, the velocity contours of the two tundish models indicate that a stronger swirling flow is generated in the rotating chamber when the outlet of the nozzle has a distance of 50 mm above the inlet of the swirling flow generator.

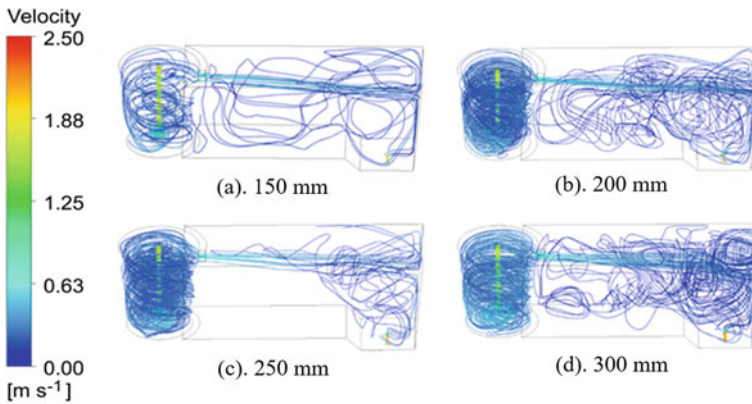**Fig. 5** Streamlines in the tundishes with different immersing depth
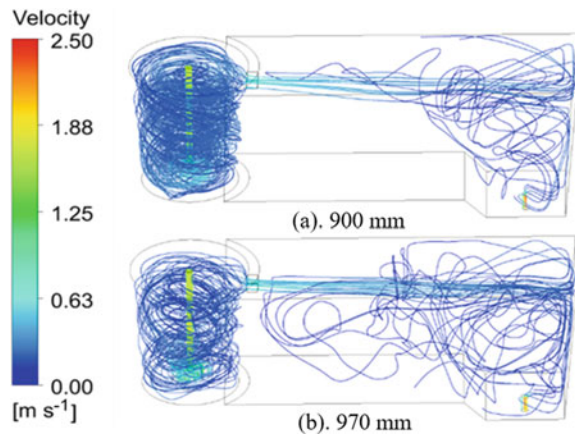
Fig. 6 Velocity contours in section A-A with different immersing depth
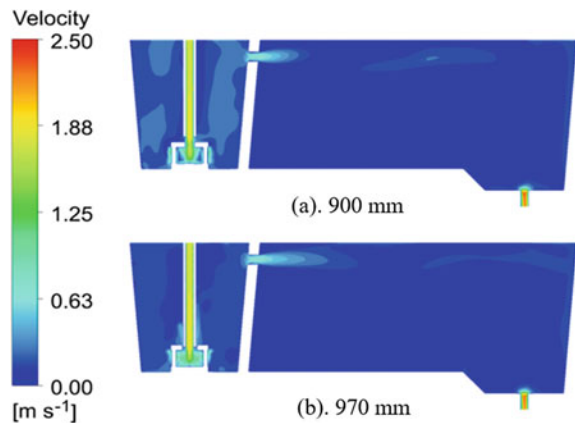
Influence of Internal Diameter

In order to determine the optimum structure, the internal diameters of the swirling flow generator were varied, (150, 200, 250 and 300 mm). The streamlines of the molten steel of each model are presented in Fig. 7. The poorest tundish performance appears when the internal diameter is 150 mm, indicating that the internal diameter is too small for the swirling flow generator to generate a sufficient swirling flow in the rotating chamber. With internal diameters of 200, 250 and 300 mm, the swirling flow generator produced a similar swirling flow in the rotating chamber. With the increase of the internal diameter, the molten steel is more likely to flow along the wall of the rotating chamber.

The velocity contours of the rotating chamber area in the position of Plane 1 and Plane 2 (See Fig. 1) are shown in Figs. 8 and 9. In Fig. 8a, the molten steel flowing
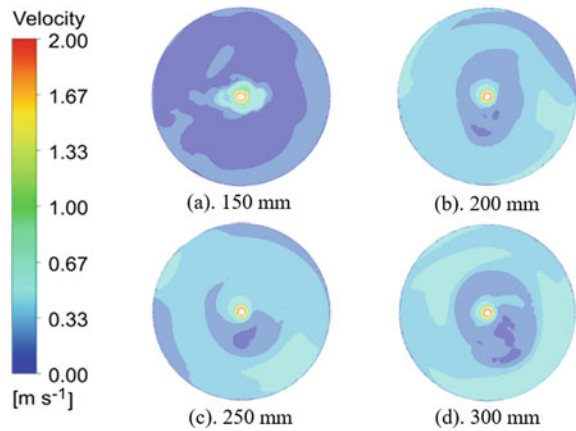

Fig. 7 Streamlines of tundishes with various sizes of swirling flow generators

Fig. 8 Velocity contours in Plane 1 in rotating chamber with different internal diameters of swirling flow generator
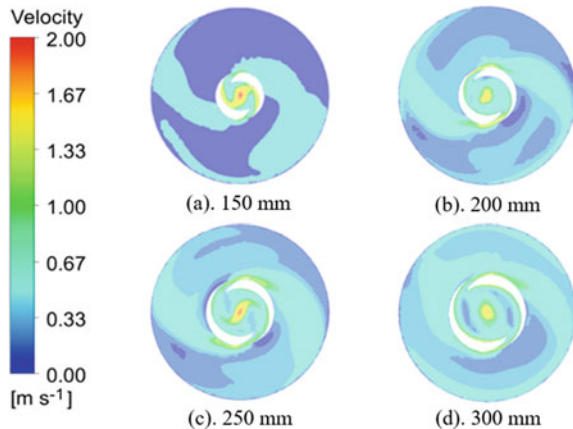
Fig. 9 Velocity contours in Plane 2 in rotating chamber with different internal diameters of swirling flow generator
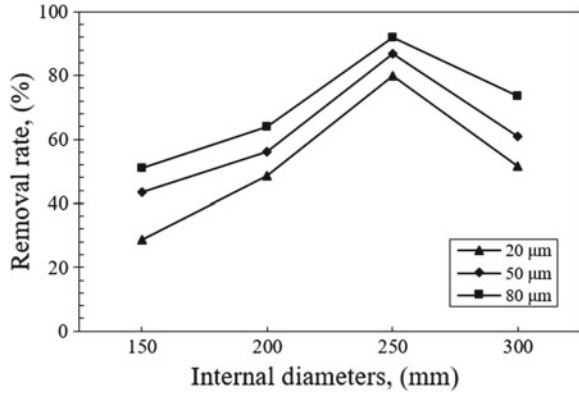

out of the tangential outlets is shown to go straight to the wall of the rotating chamber when the internal diameter of the swirling flow generator is 150 mm. Furthermore, the velocity contour at Plane 2 in Fig. 9a indicates that the kinetic energy of the molten steel is insufficient to generate a well-developed swirling flow at the upper part of the rotating chamber. By comparison with the other velocity contours, the swirling flow is well developed and symmetric in Fig. 8c; while the swirling flow is not well developed in Fig. 8b and not symmetric in Fig. 8d. Therefore, it may be concluded that the swirling flow generator with an internal diameter of 250 mm generated a relatively ideal flow field for inclusion removal.
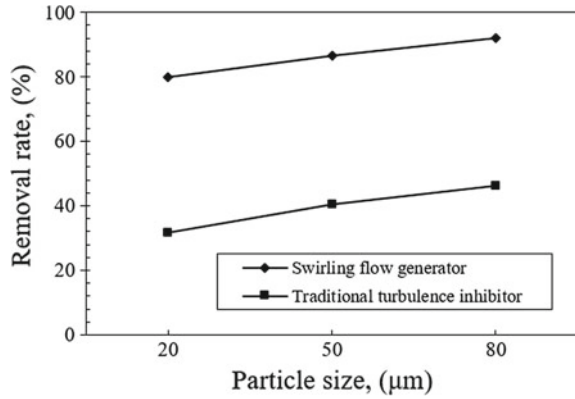
Removal of Inclusion Particles

The inclusion removal rate must be considered to find the optimum structure. Inclusion particles with diameters of 20, 50 and 80 μm were tracked and the results are presented at Fig. 10. In all models, the removal rate increased with the increasing particle size because larger inclusions are easier to float and be removed. Additionally, when the internal diameter of the swirling flow generator is less than 250 mm, the inclusion removal rate increases with increased internal diameter; while the inclusion removal decreases with the increasing of the internal diameter of the swirling flow generator when its diameter is larger than 250 mm. The model with the internal diameter of 250 mm achieves a higher removal rate than the others regardless of the inclusion size. The highest removal rate of inclusions reaches 91.9% as the inclusion size is 80 μm and the internal diameter of the swirling flow generator is 250 mm, which indicates that the optimal internal diameter is 250 mm.

The comparison of inclusion removal rates between swirling flow generator and traditional turbulence inhibitor with the internal diameter of 250 mm was investigated. The sizes of the inclusion particles are set at 20 μm 50 and 80 μm, the results

Fig. 10 Removal rates of
different inclusions

Fig. 11 Comparsion of
inclusion removal rates

of which are shown in Fig. 11. The inclusion removal rates increase with increasing
particle size for both the tundish applied with swirling flow generator and tradi-
tional turbulence inhibitor. However, the inclusion removal rate of the tundish with
swirling flow generator is double that of the traditional one for any size of inclusion
particles. The application of the swirling flow generator is feasible to significantly
strengthen the removal of inclusions.

Conclusions

A novel tundish design incorporates a swirling flow generator. The swirling flow
generator was optimized by numerical simulation. The following conclusions are
drawn from this study:

(1) By applying the swirling flow generator, a swirling flow of the molten steel is successfully generated in the rotating chamber in the tundish. The idea of swirling flow generator takes advantage of the gravitational potential energy of the molten steel to generate a swirling flow that increases the collision rate of the inclusion.

(2) The influence of the nozzle immersion depth was investigated. The patterns of streamlines indicate that the swirling flow is much stronger when the immersing depth is 900 mm that is 50 mm above the inlet of the swirling flow generator.

(3) The flow characteristics of the molten steel in the tundish with various internal diameters of the swirling flow generator were studied. The optimized internal diameter of the swirling flow generator is found to be 250 mm, in which a steady and symmetrical swirling flow is generated in rotating chamber.

(4) Inclusion particles of various size were tracked in the tundish installed a swirling flow generator with a series of internal diameters. The highest inclusion removal rate reaches 91.9% when the particle size is 80 μm and the internal diameter of the swirling flow generator is 250 mm. By comparison with traditional tundish, the swirling flow generator has the potential to significantly improve inclusion removal efficiency.

References

1. Ånmark N, Karasev A, Jönsson PG (2017) The influence of microstructure and non-metallic inclusions on the machinability of clean steels. Steel Res Int 88(1):1–10
2. Ramesha DK, Hosur KS (2013) Numerical investigation of steel grade change using ANSYS. Int J Innovative Res Sci Eng Technol 2(10):5601–5606
3. Sahai Y, Emi T (2007) Tundish technology for clean steel production. World Sci:8–11
4. Solorio-Dĺaz G, Morales RD, Ramos-Banderas A (2005) Effect of a swirling ladle shroud on fluid flow and mass transfer. Int J Heat Mass Transf 48(17):3574–3590
5. Miki Y, Ogura S, Fujii T (1996) Separation of inclusions from molten steel in a Tundish by use of a rotating electromagnetic field. Kawasaki Steel Tech Rep 35:67–73
6. Miki Y, Kitaoka H, Sakuraya T, Fujii T (2009) Mechanism of separation of inclusions from molten steel stirred with rotating electro-magnetic field. Tetsu- to- Hagane 78(3):431–438
7. Ni P, Josson L, Ersson M, Jösson PG (2017) Application of a swirling flow producer in a conventional Tundish. ISIJ Int 57(12):2175–2184
8. Tripathi A, Ajmani SK (2011) Effect of shape and flow control devices on the fluid flow characteristics in three different industrial six strand billet caster Tundish. ISIJ Int 51 (10):1647–1656
9. Hou Q, Yue Q, Wang H, Zou Z, Yu A (2008) Modelling of inclusion motion and flow patterns in swirling flow tundishes with symmetrical and asymmetrical structures. ISIJ Int 48 (6):787–792

10. Aguilar-Rodriguez CE, Ramos-Banderas JA, Torres-Alonso E, Solorio-Diaz G, Hernández-Bocanegra CA (2018) Flow characterization and inclusions removal in a slab Tundish equipped with bottom argon gas feeding. Metallurgist 61(11–12):1055–1066
11. Hou Q, Zou Z (2005) Comparison between standard and renormalization group k-ε models in numerical simulation of swirling flow Tundish. ISIJ Int 45(3):325–330
12. Launder BE, Spalding DB (1974) The numerical computational of turbulent flows. Comput Methods Appl Mech Eng 3(2):269–289